

Dual gratings interspersed on a single butterfly scale

Abigail L Ingram, Virginie Lousse, Andrew R Parker and Jean Pol Vigneron

J. R. Soc. Interface 2008 **5**, 1387-1390
doi: 10.1098/rsif.2008.0227

References

[This article cites 2 articles](#)

<http://rsif.royalsocietypublishing.org/content/5/28/1387.full.html#ref-list-1>

Article cited in:

[http://rsif.royalsocietypublishing.org/content/5/28/1387.full.html#related-urls](#)

Email alerting service

Receive free email alerts when new articles cite this article - sign up in the box at the top right-hand corner of the article or click [here](#)

To subscribe to *J. R. Soc. Interface* go to: <http://rsif.royalsocietypublishing.org/subscriptions>

REPORT

Dual gratings interspersed on a single butterfly scale

Abigail L. Ingram^{1,*}, Virginie Lousse^{2,3},
 Andrew R. Parker^{1,4} and Jean Pol Vigneron²

¹*Natural History Museum, Cromwell Road,
 London SW7 5BD, UK*

²*Département de Physique, Facultés Universitaires
 Notre-Dame de la Paix, 61 Rue de Bruxelles,
 5000 Namur, Belgium*

³*Ginzton Laboratory, Stanford University,
 Stanford, CA 94305, USA*

⁴*School of Biological Sciences, University of Sydney,
 NSW 2006, Australia*

Iridescent butterfly wing colours result from the interaction of light with sub-micrometre structures in the scales. Typically, one scale contains one such photonic structure that produces a single iridescent signal. Here, however, we show how the dorsal wings of male *Lamprolenis nitida* emit two independent signals from two separate photonic structures in the same scale. Multiple independent signals from separate photonic structures within the same sub-micrometre device are currently unknown in animals. However, they would serve to increase the complexity and specificity of the optical signature, enhancing the information conveyed. This could be important during intrasexual encounters, in which iridescent male wing colours are employed as threat displays. Blazed diffraction gratings, like those found in *L. nitida*, are asymmetric photonic structures and drive most of the incident light into one diffraction order. Similar gratings are used in spectrometers, limiting the spectral range over which the spectrometer functions. By incorporating two interchangeable gratings onto a single structure, as they are in *L. nitida*, the functional range of spectrometers could be extended.

Keywords: butterfly wing colour; iridescent signal; photonic structure; blazed diffraction grating; spectrometer

Lamprolenis nitida Godman & Salvin (1881) (Satyrinae: Nymphalidae), a New Guinean forest species (Parsons 1998), appears matt brown dorsally when illuminated and observed from above (figure 1a,b, background). However, when light is incident on the hindwing of a male in an anteroposterior direction, bright green to red iridescence is observed in backscatter (figure 1a, inset).

*Author for correspondence (a.ingram@nhm.ac.uk).

Received 27 May 2008
 Accepted 26 June 2008

If illumination and observation positions are then rotated approximately 180° on the hindwing, further backscattered iridescence from blue to violet is visible, albeit more faintly, in the same location (figure 1b, inset). Iridescence in either direction was not observed from females. Since all of the colours observed from the hindwing do not occur in the order in which we would see them together in a single spectrum, despite originating from the same region on the wing, the two signals must originate from separate photonic structures on the same scale. Typically a single photonic structure provides a single optical signal (e.g. Bálint *et al.* 2005). Multiple signals from independent photonic structures within the same sub-micrometre device are currently unknown in animals, stimulating an investigation of *L. nitida*.

Spectral measurements were taken with an Avantes Avaspec 2048/2 spectrometer. Hindwing samples were dissected from two males and adhered using double-sided tape to glass slides. The reflection was standardized using a white diffusive standard. The angle of incidence (θ) was measured from the normal to the wing sample surface and chosen to be 75° for anteroposterior illumination and 60° for posteroanterior illumination. Measurements of the anteroposterior iridescence confirmed the observed backscattered shift from green to red with observation angle getting closer to the wing surface normal (figure 1c(i)). Wavelengths below 450 nm (blue–UV) were imperceptible (even at normal incidence) as was the specular reflection. The relatively weaker iridescence visible in the posteroanterior direction also lacked specularity and shifted from blue to UV with increasing observation angle from 60° to 75° (figure 1c(ii)). Both datasets suggested the presence of blazed diffraction gratings, since these asymmetric optical devices produce correspondingly asymmetric diffraction patterns, driving most of the incident light into one diffraction order, in this case $m = -1$ (backscatter).

A section of the discal area of the hindwing was dissected from the same two males, mounted on metal stubs, coated in 15 nm of gold and viewed with a Philips XL30 scanning electron microscope at 5 kV. Observations of individual scales revealed two opposed, periodic and asymmetric structures capable of behaving as blazed gratings: the ‘cross-ribs’ (C) that connect adjacent ‘longitudinal ridges’ (Lr) and the ‘flutes’ (F) that project laterally from the ridges (figure 1d). The former are plate like, 2 µm wide by 0.5 µm deep and 100 nm thick (figure 1d,e) with a periodicity of 582 ± 12 nm ($n = 10$; figure 1e). Each cross-rib is tilted at 30° to the scale surface towards the costal margin of the hindwing (figure 1d). Individual flutes are similarly 100 nm thick; however, their periodicity is 205 ± 5 nm ($n = 10$; figure 1e) and they are tilted at 45° to the scale surface towards the outer margin of the hindwing (figure 1d).

Predicted emergent beams were calculated for both gratings using conventional diffraction theory modified to account for the 20° inclination of the scale to the wing (denoted by γ),

$$\sin(\phi + \gamma) = \sin(\theta - \gamma) + m\lambda/b, \quad (1.1)$$

where ϕ is the angle of emergence; γ is the angle between the scale and wing surfaces; θ is the angle of incidence; m is an integer indicating the diffraction

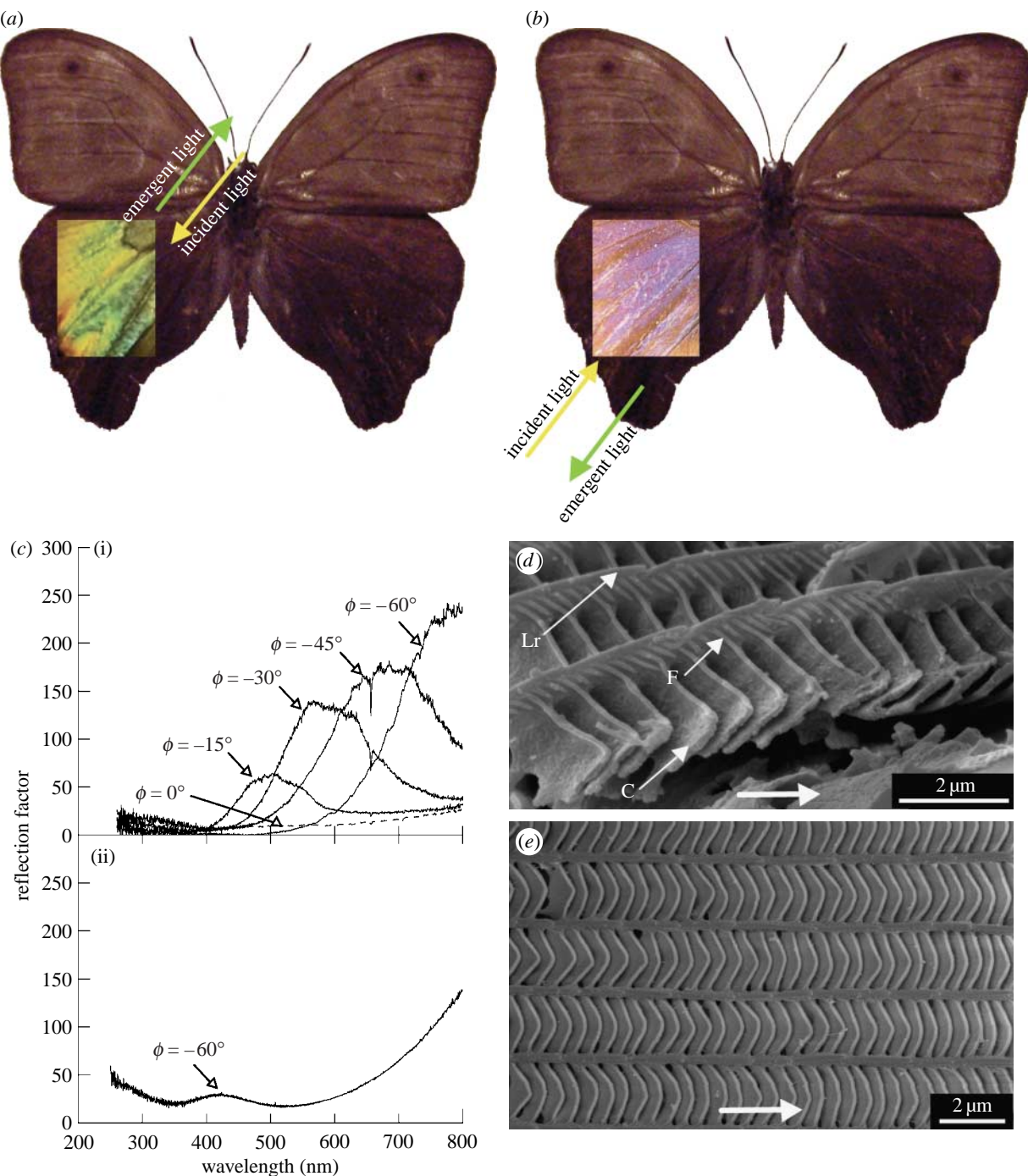


Figure 1. (a, b) The dorsal wings of male *L. nitida* appear matt brown under incident light, normal to the wing surface (background). (a) When illuminated (yellow line) in an anteroposterior direction and observed in backscatter (green line), green to red is observed with increasing angle from the wing surface (inset). (b) When illuminated in a posteroanterior direction (yellow line) and observed in backscatter (green line), blue to violet is observed with increasing angle from the wing surface (inset). (c) Backscattered (negative) emergent reflection factor as a function of wavelength (nm), recorded when the dorsal hindwing of a male *L. nitida* is illuminated (i) anteroposteriorly and (ii) posteroanteriorly and observed at an angle to the wing surface normal. Anteroposterior illumination shows the peak wavelength shift from 500 (green) to 800 nm (near IR) with increasing emergent angle (ϕ) from the wing surface. The angle of incidence (θ) was fixed at 75° . The expected peak at approximately 400–450 nm (blue-violet) was not observed at normal incidence (0°). Posteroanterior illumination shows the relatively weaker reflection and the peak at 425 nm (violet) when illumination is incident at 60° (θ) and observed at 60° (ϕ). (d) Scanning electron micrograph showing an oblique view of an individual cover scale from the dorsal hindwing of a male *L. nitida*, indicating the position of the cross-ribs (C), flutes (F) and longitudinal ridges (Lr). The thick arrow indicates the direction towards the costal margin. (e) Scanning electron micrograph showing a plan view of an individual cover scale from the dorsal hindwing of a male *L. nitida*, from which measurements were taken of the grating period. The arrow indicates the direction towards the costal margin.

order; λ is the wavelength of light; and b is the grating period. In each case, the beams were restricted to $m = -1$ (figure 2a, b), matching experimental data.

To investigate the absence of wavelengths under 450 nm from the anteroposterior reflection, the reflected field intensity was calculated using

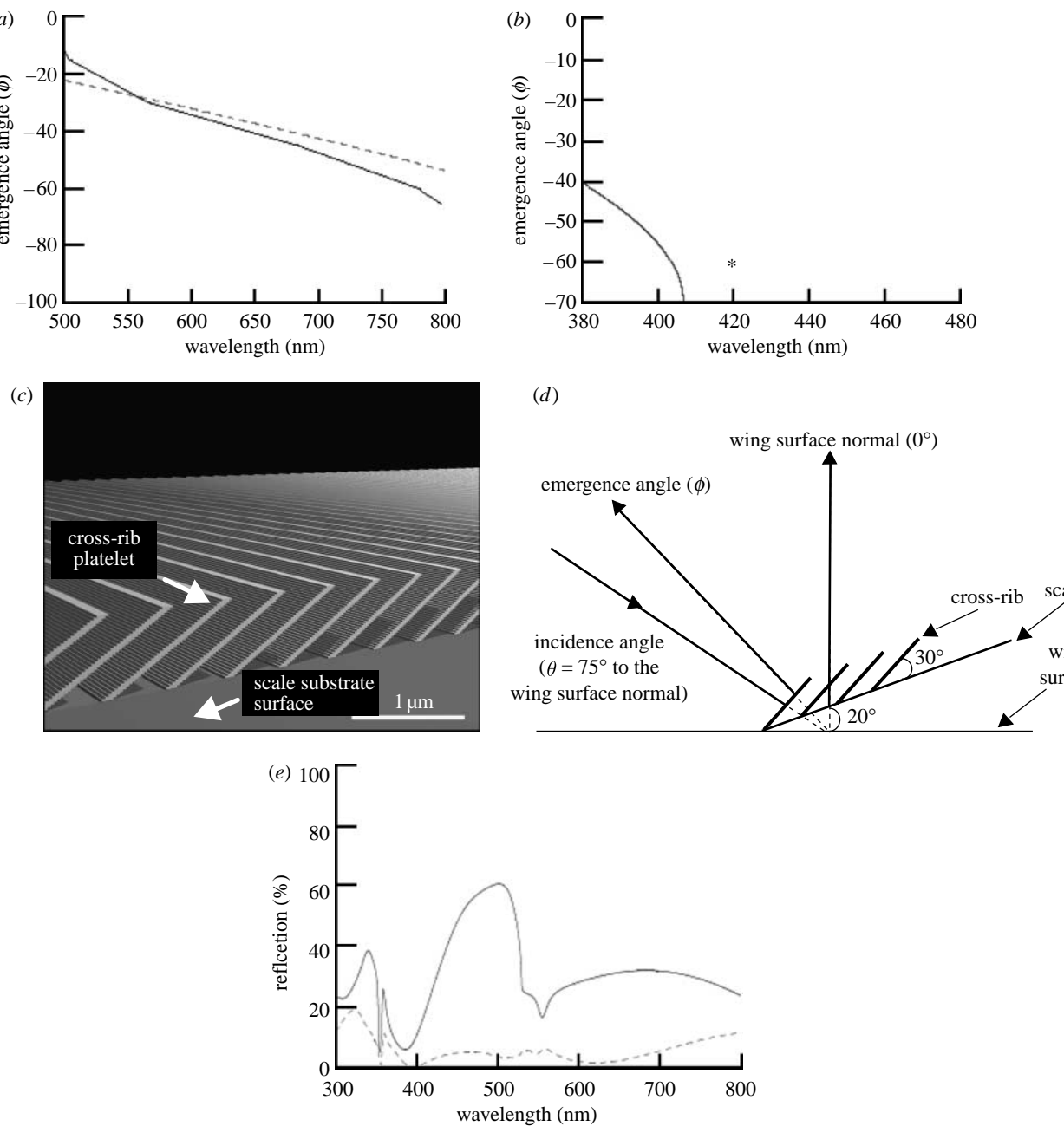


Figure 2. (a) The theoretical (dashed line) and experimental (solid line) emergence angles as a function of incident wavelength for anteroposterior illumination on the dorsal hindwing of a male *L. nitida* (incident angle fixed at 75° (θ) to the wing surface normal). Theoretical calculations were made using conventional diffraction theory modified to account for the angle, $\gamma=20^\circ$, between the surfaces of the scale and the wing. (b) The theoretical (solid line) and experimental (asterisk) emergence angles as a function of incident wavelength for posteroanterior illumination on the dorsal hindwing of a male *L. nitida* (incident angle fixed at 60° (θ) to the wing surface normal). Theoretical calculations were made using conventional diffraction theory modified to account for the angle, $\gamma=20^\circ$, between the surfaces of the scale and the wing. (c) Model of the blazed grating used to calculate the reflected field intensity from the cross-rib plates (indicated by arrow). The scale substrate (indicated by arrow) is made of chitin, containing phenomelanin. The chitinous grating platelets, tilted at 30° , are repeated at intervals of 582 nm along the substrate surface, in the direction normal to the platelets. The height (normal to the substrate surface) of the platelet layer is 672 nm. (d) Diagram showing the relative positions and angles of the cross-ribs, scale and wing membrane with respect to one another. (e) Computed reflected field intensity of the cross-rib grating using the multiple scattering transfer-matrix approach, restricted to the specular beam (dashed, $m=0$) and including all diffracted beams (here, only one beam, $m=-1$, besides the specular $m=0$). The angle of incidence from the normal to the scale is 55° . The residual reflectance in the specular direction is due to the presence of an absorbing substrate: the extinction of this $m=0$ beam benefiting the $m=-1$ order is due to the asymmetric blazed profile of the grooves.

the multiple scattering transfer-matrix approach (Pendry & Mackinnon 1992; Vigneron & Lousse 2006). A model of the grating was composed of a flat semi-infinite chitin substrate containing phenomelanin

(Fox 1953), representing the scale (figure 2c). The substrate was terminated by a planar surface and the cross-ribs, constituting the grating, were represented by platelets tilted at 30° from the substrate surface. The

total height of the platelets was 672 nm. The period containing one cross-rib (582 nm) was repeated along the substrate surface plane, forming a grating composed of an array of parallel ribbons. The incident beam was launched at 75° to the wing surface (figure 2d) towards the platelet slope, as required to use the blazed grating. Owing to the inclination of the scale to the wing surface, the incidence angle was reduced by 20° (figure 2d), giving an adjusted incidence angle of 55° for the calculation. The three-dimensional multiple scattering of fully vectorial electromagnetic waves in this complex structure was treated layer by layer, and the outgoing intensities of the specular and the first-order diffraction beams were evaluated by assembling scattering matrices. The specular reflection was relatively uniform, characteristic of a strongly desaturated colour (figure 2e). This spectrum was nearly identical to that obtained when inverting the light path, or reversing the slope of the platelets, indicating that it was not associated with the grating, but is a reflectance from the flat substrate. The associated reflectance was weak because the substrate incorporates absorbing melanin. The total diffracted energy, including the $m = -1$ beam, is stronger than the specular reflectance and vanishes if the light path is reversed, confirming again the presence of a blazed grating. The model predicted the decreasing intensity of the diffraction beam at approximately 450 nm (figure 2e), as observed from the anteroposterior spectrum. This is thought to be due to the extended height of the cross-ribs, restricting the angular spread of diffracted light.

The study has revealed that male *L. nitida* can emit two independent signals from two separate blazed gratings, interspersed on single scales and formed by the cross-ribs and flutes. Multiple signals increase the complexity and specificity of the optical signature, thus enhancing the information conveyed. This could be particularly important during intrasexual encounters, in which iridescent male wing colours are employed as threat displays (Silberglied 1984; Wiklund 2003). The signal would be effective in terms of the ambient light conditions found in the forest habitat of *L. nitida*, where illumination levels are generally low, with shafts of light intermittently breaking through the overhead canopy (Parsons 1998). Here, a bright directional signal would flash whenever a light shaft was encountered, making it very noticeable. In addition, forests are often species-rich habitats: a complex signal would enable *L. nitida* conspecifics to readily identify one another.

The double grating of *L. nitida* could provide a solution to a problem with spectrometers, namely that the functional range of their grating is restricted, so that when the spectral limit is reached the grating must be mechanically swapped for another, interrupting measurements. By incorporating two gratings onto a single self-adjusting surface, this problem may be circumvented.

Funding was provided by the European BioPhot (NEST) project (no. 12915), the EU5 Centre of Excellence ICAI-CT-2000-70029 and from the Inter-University Attraction Pole (IUAP P5/1) on 'Quantum-size effects in nanostructured materials' of the Belgian Office for Scientific, Technical and Cultural Affairs. The work was also partly supported by the European Regional Development Fund (ERDF) and the Walloon Regional Government under the 'PREMIO' INTERREG IIIa project. V.L. and A.R.P. were supported by the Belgian National Fund for Scientific Research (FNRS) and the Royal Society, respectively. We thank A. Lucas (FUNDP) for helpful discussions and P. Ackery (NHM, London) for butterfly specimens, and acknowledge the use of Namur Inter-University Scientific Computing Facility (Namur-ISCF) for the numerical simulations.

REFERENCES

Bálint, Zs., Vértesy, Z. & Biró, L. P. 2005 Microstructures and nanostructures of high Andean *Penaincisalia* lycaenid butterfly scales (Lepidoptera: Lycaenidae): descriptions and interpretations. *J. Nat. Hist.* **39**, 2935–2952. ([doi:10.1080/00222930500140629](https://doi.org/10.1080/00222930500140629))

Fox, D. L. 1953 *Animal biochromes and structural colours*. Cambridge, UK: Cambridge University Press.

Parsons, M. 1998 *The butterflies of Papua New Guinea: their systematics and biology*. San Diego, CA: Academic Press.

Pendry, J. B. & MacKinnon, A. 1992 Calculation of photon dispersion relations. *Phys. Rev. Lett.* **69**, 2772–2775. ([doi:10.1103/PhysRevLett.69.2772](https://doi.org/10.1103/PhysRevLett.69.2772))

Silberglied, R. 1984 Visual communication and sexual selection among butterflies. In *The biology of butterflies* (eds R. I. Vane-Wright & P. R. Ackery), pp. 207–410. London, UK: Academic Press.

Vigneron, J. P. & Lousse, V. 2006 Colored reflections from the black-billed magpie feathers. In *Proc. SPIE, Photonic Crystal Materials and Devices IV. The Nature of Light: Light in Nature*, vol. 6285 (ed. K. Creath), pp. 628–508.

Wiklund, C. 2003 Sexual selection and the evolution of butterfly mating systems. In *Butterflies: ecology and evolution taking flight* (eds C. L. Boggs, W. B. Watt & P. R. Ehrlich), pp. 67–90. Chicago, IL: The University of Chicago Press.